

International Journal of Physical Sciences

Volume 9 Number 11 16 June, 2014

ISSN 1992-1950



*Academic
Journals*

ABOUT IJPS

The **International Journal of Physical Sciences (IJPS)** is published weekly (one volume per year) by Academic Journals.

International Journal of Physical Sciences (IJPS) is an open access journal that publishes high-quality solicited and unsolicited articles, in English, in all Physics and chemistry including artificial intelligence, neural processing, nuclear and particle physics, geophysics, physics in medicine and biology, plasma physics, semiconductor science and technology, wireless and optical communications, materials science, energy and fuels, environmental science and technology, combinatorial chemistry, natural products, molecular therapeutics, geochemistry, cement and concrete research, metallurgy, crystallography and computer-aided materials design. All articles published in IJPS are peer-reviewed.

Contact Us

Editorial Office: ijps@academicjournals.org

Help Desk: helpdesk@academicjournals.org

Website: <http://www.academicjournals.org/journal/IJPS>

Submit manuscript online <http://ms.academicjournals.me/>

Editors

Prof. Sanjay Misra

*Department of Computer Engineering, School of Information and Communication Technology
Federal University of Technology, Minna,
Nigeria.*

Prof. Songjun Li

*School of Materials Science and Engineering,
Jiangsu University,
Zhenjiang,
China*

Dr. G. Suresh Kumar

*Senior Scientist and Head Biophysical Chemistry
Division Indian Institute of Chemical Biology
(IICB)(CSIR, Govt. of India),
Kolkata 700 032,
INDIA.*

Dr. Remi Adewumi Oluyinka

*Senior Lecturer,
School of Computer Science
Westville Campus
University of KwaZulu-Natal
Private Bag X54001
Durban 4000
South Africa.*

Prof. Hyo Choi

*Graduate School
Gangneung-Wonju National University
Gangneung,
Gangwondo 210-702, Korea*

Prof. Kui Yu Zhang

*Laboratoire de Microscopies et d'Etude de
Nanostructures (LMEN)
Département de Physique, Université de Reims,
B.P. 1039. 51687,
Reims cedex,
France.*

Prof. R. Vittal

*Research Professor,
Department of Chemistry and Molecular
Engineering
Korea University, Seoul 136-701,
Korea.*

Prof Mohamed Bououdina

*Director of the Nanotechnology Centre
University of Bahrain
PO Box 32038,
Kingdom of Bahrain*

Prof. Geoffrey Mitchell

*School of Mathematics,
Meteorology and Physics
Centre for Advanced Microscopy
University of Reading Whiteknights,
Reading RG6 6AF
United Kingdom.*

Prof. Xiao-Li Yang

*School of Civil Engineering,
Central South University,
Hunan 410075,
China*

Dr. Sushil Kumar

*Geophysics Group,
Wadia Institute of Himalayan Geology,
P.B. No. 74 Dehra Dun - 248001(UC)
India.*

Prof. Suleyman KORKUT

*Duzce University
Faculty of Forestry
Department of Forest Industrial Engineering
Beciyorukler Campus 81620
Duzce-Turkey*

Prof. Nazmul Islam

*Department of Basic Sciences &
Humanities/Chemistry,
Techno Global-Balurghat, Mangalpur, Near District
Jail P.O: Beltalpark, P.S: Balurghat, Dist.: South
Dinajpur,
Pin: 733103,India.*

Prof. Dr. Ismail Musirin

*Centre for Electrical Power Engineering Studies
(CEPES), Faculty of Electrical Engineering, Universiti
Teknologi Mara,
40450 Shah Alam,
Selangor, Malaysia*

Prof. Mohamed A. Amr

*Nuclear Physic Department, Atomic Energy Authority
Cairo 13759,
Egypt.*

Dr. Armin Shams

*Artificial Intelligence Group,
Computer Science Department,
The University of Manchester.*

Editorial Board

Prof. Salah M. El-Sayed

*Mathematics. Department of Scientific Computing,
Faculty of Computers and Informatics,
Benha University. Benha ,
Egypt.*

Dr. Rowdra Ghatak

*Associate Professor
Electronics and Communication Engineering Dept.,
National Institute of Technology Durgapur
Durgapur West Bengal*

Prof. Fong-Gong Wu

*College of Planning and Design, National Cheng Kung
University
Taiwan*

Dr. Abha Mishra.

*Senior Research Specialist & Affiliated Faculty.
Thailand*

Dr. Madad Khan

*Head
Department of Mathematics
COMSATS University of Science and Technology
Abbottabad, Pakistan*

Prof. Yuan-Shyi Peter Chiu

*Department of Industrial Engineering & Management
Chaoyang University of Technology
Taichung, Taiwan*

Dr. M. R. Pahlavani,

*Head, Department of Nuclear physics,
Mazandaran University,
Babolsar-Iran*

Dr. Subir Das,

*Department of Applied Mathematics,
Institute of Technology, Banaras Hindu University,
Varanasi*

Dr. Anna Oleksy

*Department of Chemistry
University of Gothenburg
Gothenburg,
Sweden*

Prof. Gin-Rong Liu,

*Center for Space and Remote Sensing Research
National Central University, Chung-Li,
Taiwan 32001*

Prof. Mohammed H. T. Qari

*Department of Structural geology and remote sensing
Faculty of Earth Sciences
King Abdulaziz UniversityJeddah,
Saudi Arabia*

Dr. Jyhwen Wang,

*Department of Engineering Technology and Industrial
Distribution
Department of Mechanical Engineering
Texas A&M University
College Station,*

Prof. N. V. Sastry

*Department of Chemistry
Sardar Patel University
Vallabh Vidyanagar
Gujarat, India*

Dr. Edilson Ferneda

*Graduate Program on Knowledge Management and IT,
Catholic University of Brasilia,
Brazil*

Dr. F. H. Chang

*Department of Leisure, Recreation and Tourism
Management,
Tzu Hui Institute of Technology, Pingtung 926,
Taiwan (R.O.C.)*

Prof. Annapurna P.Patil,

*Department of Computer Science and Engineering,
M.S. Ramaiah Institute of Technology, Bangalore-54,
India.*

Dr. Ricardo Martinho

*Department of Informatics Engineering, School of
Technology and Management, Polytechnic Institute of
Leiria, Rua General Norton de Matos, Apartado 4133, 2411-
901 Leiria,
Portugal.*

Dr Driss Miloud

*University of mascara / Algeria
Laboratory of Sciences and Technology of Water
Faculty of Sciences and the Technology
Department of Science and Technology
Algeria*

ARTICLES

- Markov chain model for the dynamics of cooking fuel usage:
Transition matrix estimation and forecasting** 255
Garba S. Adamu and Danbaba A.
- Studies on zinc oxide thin films by chemical spray pyrolysis technique** 261
Prabakaran Kandasamy and Amalraj Lourdusamy
- Kinematics of the human hand applied to the design of prosthesis** 267
Luis Antonio Aguilar-Pérez, Christopher René Torres-San Miguel,
Guillermo Urriolagoitia-Sosa, Luis Martínez-Sáez, José Alfredo Leal-Naranjo,
Beatriz Romero-Ángeles and Guillermo Urriolagoitia-Calderón

Full Length Research Paper

Markov chain model for the dynamics of cooking fuel usage: Transition matrix estimation and forecasting

Garba S. Adamu^{1*} and Danbaba A.²

¹Department of Mathematics, Waziri Umaru Federal Polytechnic, Birnin Kebbi, Nigeria.

²Department of Statistics, Usmanu Danfodiyo University, Sokoto, Nigeria.

Received 12 March, 2014; Accepted 28 May, 2014

Markov chain models are valuable tools for modeling data that vary over time. They are suitable models to use when modeling the transitions of variables between discrete states over time. In this paper, Markov chain model was applied to the data obtained from 300 households living in the headquarters of three Local Governments (Argungu, Arewa, and Augie) of Kebbi State, Nigeria. The data was information concerning the main source of fuel for cooking used by each of the households. The types of fuels were; fuel-wood, gas, kerosene and electricity. The initial distribution of the households was obtained based on the information in December, 2010 which was used as a baseline. Thereafter, the subsequent data for 2011, 2012 and 2013 were labeled as Periods 1, 2 and 3, respectively. Using this procedure, a transition matrix for the households was obtained and analyzed using Markov chain model. The model was implemented using R-statistical software version 3.0.2. The results obtained indicate a high probability of increase in the use of wood as fuel for cooking by the households. The probability of using other alternative fuels diminishes over time.

Key words: Households, cooking fuel, Markov chains, transition probability.

INTRODUCTION

According to Thierauf and Klekamp (1975), Markov chains originated with the studies of Markov (1906 - 1907) on the sequence of experiments connected in a chain, and with attempts to describe mathematically the physical phenomenon known as Brownian motion. In many real world problems, it is convenient to classify individuals or items into distinct categories or states. We can then analyze the transitions of these individuals or items from one state to another over time (Elwood and James, 1978). Markov chains is a method of studying changes in state of variables with respect to changes in time, in an effort to predict the future state of those

variables (Richard and Charles, 1975). According to Sung et al. (2004) and Welton and Ades (2005), Markov chain models are useful tools for modeling data that vary over time. Markov models are appropriate for the analysis of problems in marketing, income tax auditing, car rental services, inventory, machine maintenance and replacement, stock market analysis and hospital administration (Kannan and Lakshmikanthan, 2002). Markov chain model is a suitable model to use when modeling the transitions of patients between discrete health states over time especially the progression over stages of a disease (McDonnel et al., 2002;

*Corresponding author. E-mail: abujabaka2@yahoo.com, Tel: +2348063496230.

Author(s) agree that this article remain permanently open access under the terms of the [Creative Commons Attribution License 4.0 International License](http://creativecommons.org/licenses/by/4.0/)

Meredith, 1976). Sonnenberg and Beck (1993) applied Markov model in the prognosis of clinical problems. They modeled the events of interest as transition from one state to another.

Fuel is indispensable to human existence for warmth and food preparation. There are different ways a man obtains his required fuel; among these is the fuel-wood. It was approximated that 2.5 to 3.0 billion people rely on wood for fuel. Wood accounts for up to 58% of all energy requirements in African savanna areas (Williams, 2003). Personal interviews and observations indicate that majority of households in Argungu, Arewa and Augie Local Government headquarters are dependent on fuel-wood for cooking. This may not be unconnected to lack of inter-fuel substitution for household choice and the use of a given source of fuel, depend on socio-economic (e.g. family income), demographic (e.g. family size, household composition, life style and culture) and location attributes (e.g. proximity to sources of modern and traditional fuels) (Ayotebi, 2000; Adebaw, 2007).

The use of fuel-wood in Nigeria greatly contributes to desert encroachment and consequently has implications with regard to climate change. Upon this, a little comes to light about the drives and dynamics of fuel-wood consumption in Nigeria (Adebaw, 2007). For the purpose of this research, a household is defined as group of persons living together and maintaining unique eating arrangement. The head of a household is responsible for proving the necessities in the household (NBS, 2012).

MATERIALS AND METHODS

Data collection

In this research, the population was the entire households in the three Local Government headquarters (Argungu, Arewa, and Augie) of Kebbi State, Nigeria. A convenience sampling technique was used to select a sample of 300 households that use one of the common types of fuel as their major source of energy for cooking were interviewed for the purpose of determining and predicting the dynamics of fuel use for the period of 3 years (2010 to 2013). However, the selection of the sample was guided by National Bureau of Statistics Report (NBS, 2012). The detail of the sample was Argungu 185, Augie 50, and Arewa 65 households. The respondents were asked questions pertaining their main source of fuel for cooking among the following categories; A (fuel-wood), B (cooking gas), C (kerosene) and D (electricity).

Analytical technique

For the purpose of this research, Markov chain is used in the prediction of households' choice of means of fuel for cooking in the three Local Government headquarters of Kebbi State, Nigeria. A stochastic process is regarded as a sequence of random variables over time. A random variable taking one of the values 1, 2, 3 ... *k* is associated with each point and the sequence is determined by Markov chain with transition matrix *P* (Tijms, 2003; Hsu, 1997; Schuss, 2010; Cox and Isham, 1980; Norris, 1997; Bailey, 1964). The sequence of number of household that use a particular fuel type is considered to be a realization of a stochastic process. If *X_t*

denotes the number of households that maintain the use of a particular fuel for a given period, *X_t* is a random variable describing the outcome of the fuel usage on the *tth* period and is termed as "the state" of the process. In Markov process, the probability of moving from one state to another depends only on the present state and not the history.

According to Sung et al. (2006), they defined {*S_{m0}, S_{m1}, ..., S_m*} as a sequence of random variables indexed by time, taking finite values in $\mathcal{E} = \{1, \dots, J\}$. Assume that the sequence {*S_{m0}, S_{m1}, ..., S_m*} forms a first order Markov chains as the conditional probability distribution of *S_{mt}* given *S_{m,t-1}, ..., S_{m,0}* depend only on the value of *S_{m,t-1}*. Let *X_{ij}(t)* represents the transition from state *i* at time (*t - 1*) to state *j* at time *t*. Let a matrix of state transition probabilities be defined where each row entry represents an initial state and each column entry represents a destination state. That is,

$$X(t) = \begin{bmatrix} x_{11}(t) & \dots & x_{1M}(t) \\ \vdots & \ddots & \vdots \\ x_{M1}(t) & \dots & x_{MM}(t) \end{bmatrix} \tag{1}$$

Where

$$\sum x_{ij} = 1. \tag{2}$$

And *x_{ij}* is defined as

$$x_{ij} = \Pr(X_n = j | X_{n-1} = i) \tag{3}$$

More generally, let *n_{ij}* denote the number of individuals who were in state *i* in period *t-1* and are in state *j* in period *t*. The probability of an individual being in state *j* in period *t* given that they were in state *i* in period *t-1*, denoted by *x_{ij}*, can be estimated using the following formula:

$$x_{ij} = \frac{n_{ij}}{\sum_j n_{ij}} \tag{4}$$

Thus, the probability of transition from any given state *i* is equal to the proportion of individuals that started in state *i* and ended in state *j* as a proportion of all individuals in that started in state *i*. According to Hsu (1997), Bailey (1964) and Ross (2007), the Markov chain described above has an initial probability vector

$$X_0 = (i_1, i_2, i_3, \dots, i_n) \tag{5}$$

i's are the states and transition matrix *X_{ij} = P*, the probability vector after *n* repetitions of the experiment is

$$V = X_0 P^n \tag{6}$$

That is, for any regular transition matrix *P*, there is a unique vector *V* such that for any probability vector *X₀* and for large value of *n*,

Table 1. Initial distribution of households over the states ($t = 0$).

State	Number of households	Percentage
A	278	92.7
B	11	3.6
C	9	3.0
D	2	0.7

$V = X_0 P^n$. Vector V is called the equilibrium vector of the Markov chain. From the above fact, and for large value of n ,

$$\begin{aligned} X_0 \cdot P^n \cdot P &= V \cdot P \\ X_0 \cdot P^{n+1} &= VP \end{aligned} \tag{7}$$

as $n \rightarrow \infty, X_0 \cdot P^n \rightarrow V$ so that $X_0 \cdot P^{n+1} \rightarrow VP \rightarrow V$, (Danbaba and Isah, 2002). Moreover, at equilibrium, Equation 8 represents the proportion of the households in each state.

$$\lim_{n \rightarrow \infty} P^n = W \left(\lim_{n \rightarrow \infty} \Lambda^n \right) W^{-1} = L \tag{8}$$

Where P is the matrix of transition probabilities, W and Λ are matrices of the eigenvectors and eigenvalues of P , respectively and the rows of L are all the same. (Burley and O'sullivan, 1986; Ross, 2007).

Basic assumptions

It is assumed in this paper that;

- a) Markov process is homogeneous and finite,
- b) The number of fuel types (states) remain constant, that is, no new type of fuel used by the selected households,
- c) Households used only one of the fuels at a regular interval, that is, yearly in this case.
- d) No household leave the system throughout the periods of this research.

RESULTS AND DISCUSSION

At the beginning of data collection, at $t = 0$, there were a total of 300 households, out of which 278 or 92.7% were in Atate A (fuel-wood), 11 household or 3.6% were in State B (gas), 9 households or 3.0% were in State C (kerosene) and only 2 households or 0.7% use electricity as main source of fuel for cooking, that is State D. (Table 1). Table 2 summarizes the flow of fuel users from one type of cooking fuel to another from December, 2010 to December, 2013.

Transition matrix

	A	B	C	D
A	0.9882	0.0083	0.0035	0
P = B	0.4643	0.3214	0.1786	0.0357
C	0.3636	0.1818	0.4546	0
D	0.2500	0.5000	0	0.2500

(9)

The information in Table 2 is more useful when transformed into a transition probability matrix (9). To calculate the entries in the matrix, we sum up (say A to A for example) values and divide it by the row total ($\frac{836}{846} = 0.9882$). Continuing in this manner for other

transition routes, we obtained a one-step transition matrix (9). The probabilities of the household moving from state A to States B, C and D are 0.0083, 0.0035 and 0, respectively. In other words, after one-step, the chance of making transition from fuel-wood to gas and kerosene is low. There is no chance of moving from fuel-wood to electricity. The probability of the household remaining in State A (continue using wood for cooking) is as high as 0.9882. The probability of making a forward transition (i.e., Wood \rightarrow gas \rightarrow kerosene \rightarrow electricity) is low while the probability of making backward transition (that is, Wood \leftarrow gas \leftarrow kerosene \leftarrow electricity) is high. The chance of abandoning the use of cooking gas for wood is relatively high (0.5). The chances of abandoning kerosene and electricity for wood are 0.4 and 0.3, respectively. Also, the chance of leaving electricity for gas is good (0.5). The tendency of the household to continue with the use of cooking gas, kerosene and electricity is 0.3, 0.5 and 0.3, respectively. Most importantly, the probability of leaving the use of wood for cooking for its alternative is approximately 0.

Transition diagram

Figure 1 shows a one step transition diagram. It shows the movement of households from one type of cooking fuel to another.

In 2011, 4 households migrate from wood to gas, one from wood to kerosene and none from wood to electricity. Five (5) moved from gas to wood, 1 each from gas to kerosene and electricity. Four households move from using kerosene to fuel-wood, 1 kerosene to gas, and none move from kerosene to electricity. One household moves from electricity to gas, and no other movement from electricity to other fuel types. The same explanation follows in 2012 and 2013. At the end of the data collection, the distribution of the households over the states changed as follows; 290 or 96.6% wood, 5 or 1.7% gas, and 5 or 1.7% kerosene.

To compute fuel shares of the households for a

Table 2. Flow of households from one type of cooking fuel to another (2010 - 2013)

State	December 2010	2011				2012				2013				December 2013
		A	B	C	D	A	B	C	D	A	B	C	D	
A	278	273	4	1	0	278	2	2	0	285	1	0	0	290
B	11	5	4	1	1	5	2	3	0	3	3	1	0	5
C	9	4	1	4	0	2	2	2	0	2	1	4	0	5
D	2	0	1	0	1	1	1	0	0	0	0	0	0	0

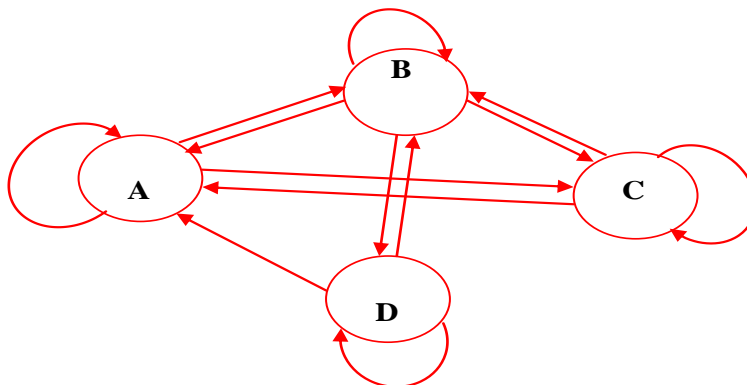


Figure 1. Transition diagram showing the possible transitions.

Table 3. Fuel shares from December, 2010 to December, 2022.

Year	Period	Fuel shares of the households (%)			
		A	B	C	D
2010	1	98.82	0.83	0.35	0.00
2011	2	98.17	1.15	0.65	0.03
2012	3	97.79	1.31	0.85	0.05
2013	4	97.57	1.41	0.96	0.06
2014	5	97.43	1.47	1.03	0.07
2015	6	97.36	1.50	1.07	0.07
2016	7	97.31	1.52	1.10	0.07
2017	8	97.29	1.53	1.11	0.07
2018	9	97.27	1.54	1.12	0.07
2019	10	97.26	1.54	1.12	0.07
2020	11	97.25	1.54	1.13	0.07
2021	12	97.25	1.54	1.13	0.07
2022	13	97.25	1.55	1.13	0.07

Particular year, matrix P and the fuel shares of the preceding year are required. The household-shares of the four competing fuel types for the periods of December, 2010 to December, 2022 have been summarized in Table 3. The table indicates that if the present trends continue for instance, fuel-wood will have 97.25% of the households in the year 2020, while gas,

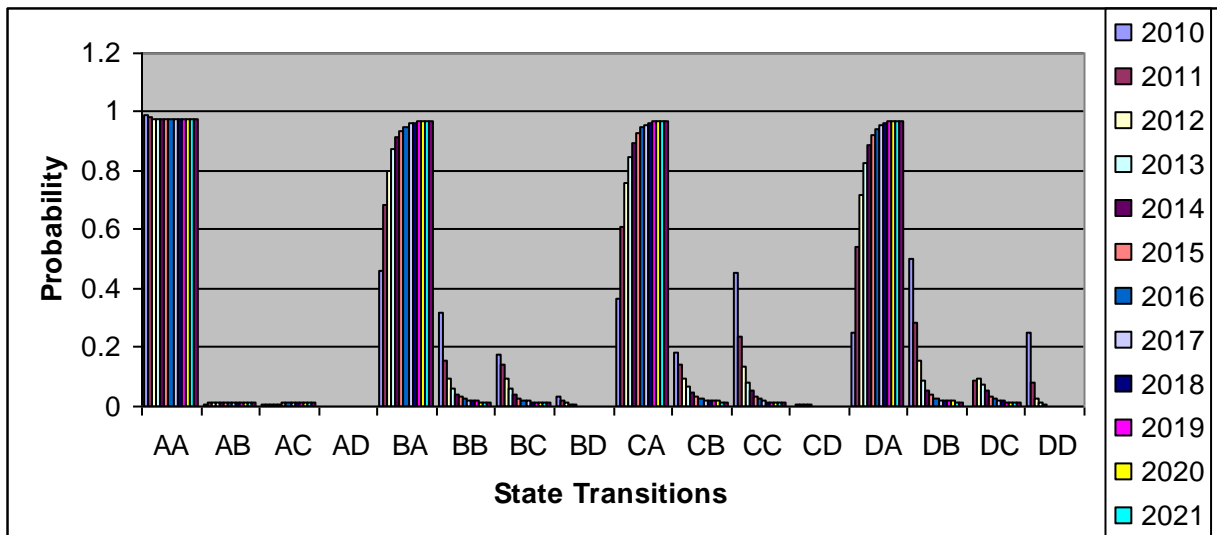
kerosene and electricity will have 1.54, 1.13 and 0.07%, respectively.

Prediction of fuel usage by the households

Applying equation 6 to the initial probability vector

Table 4. Projection of transition probabilities for 13 years (2010 to 2022).

State	2010	2011	2012	2013	2014	2015	2016	2017	2018	2019	2020	2021	2022
AA	0.988	0.982	0.978	0.975	0.974	0.973	0.973	0.973	0.973	0.973	0.973	0.973	0.973
AB	0.008	0.012	0.013	0.014	0.015	0.015	0.015	0.015	0.015	0.015	0.015	0.015	0.015
AC	0.004	0.007	0.008	0.010	0.010	0.011	0.011	0.011	0.011	0.011	0.011	0.011	0.011
AD	0.000	0.000	0.001	0.001	0.001	0.001	0.001	0.001	0.001	0.001	0.001	0.001	0.001
BA	0.464	0.682	0.803	0.873	0.914	0.938	0.952	0.961	0.966	0.968	0.970	0.971	0.971
BB	0.321	0.157	0.092	0.059	0.040	0.031	0.024	0.020	0.018	0.017	0.016	0.016	0.016
BC	0.179	0.140	0.094	0.062	0.042	0.029	0.022	0.018	0.015	0.014	0.013	0.012	0.012
BD	0.036	0.020	0.011	0.006	0.004	0.002	0.002	0.001	0.001	0.001	0.001	0.001	0.001
CA	0.363	0.609	0.758	0.846	0.898	0.929	0.947	0.957	0.964	0.967	0.969	0.971	0.971
CB	0.182	0.144	0.098	0.066	0.046	0.033	0.026	0.022	0.019	0.018	0.017	0.016	0.016
CC	0.455	0.240	0.137	0.083	0.052	0.035	0.025	0.020	0.016	0.014	0.013	0.012	0.012
CD	0.000	0.007	0.007	0.005	0.004	0.003	0.002	0.001	0.001	0.001	0.001	0.001	0.001
DA	0.250	0.542	0.722	0.826	0.887	0.923	0.944	0.955	0.962	0.967	0.969	0.971	0.971
DB	0.500	0.288	0.154	0.088	0.055	0.038	0.028	0.023	0.020	0.018	0.017	0.016	0.016
DC	0.000	0.090	0.094	0.073	0.052	0.036	0.026	0.020	0.017	0.014	0.013	0.012	0.012
DD	0.250	0.080	0.030	0.013	0.006	0.003	0.002	0.002	0.001	0.001	0.001	0.001	0.001

**Figure 2.** Projection of transition probabilities of moving to each state from 2010 to 2022.

described in Table 1, that is,

$X_0 = (0.927 \ 0.036 \ 0.030 \ 0.007)$ and Transition matrix (9), the projected transition probabilities in Table 4 were obtained. Table 4 gives the projection of transition probabilities for 13 years (that is, 2010 to 2022).

Figure 2 is a graphical representation of the four competitive fuel type's transition probabilities for the periods under study. The transition probability of the fuels decreases over the years in favor of the fuel-wood. That is, the probability of the households using gas, kerosene and electricity reduces steadily over the years. The probability of preference of the fuel-wood over other

types of fuels for cooking increases across the years. In other words, the probability of the households moving from gas to wood, kerosene to wood and electricity to wood increases steadily over the years. The hope for the households changing cooking fuel from fuel-wood to its alternative is very little. Eventually, all the transition probabilities remain constant in 2021 that is after 12 years.

Conclusion

This paper used Markov chain model to analyze the

behavior of the households in respect of using four types of fuel for cooking in three local government headquarters of Kebbi State, Nigeria. Three years observation periods were used and transition probabilities were calculated up to equilibrium stage. At that state, it is predicted that the probability of households using wood as fuel for cooking is 0.971. This means 97.1% of the household will use wood as their main source of fuel for cooking in the year 2022. This is a sharp increase of fuel-wood users on the initial figure of 92.7%. The probability of the households using gas for cooking is 0.016 or only 1.6% of the households will use gas for cooking,

indicating a sharp decline from the initial figure 3.6%. The same situation was observed for kerosene and electricity declining from 3.0 and 0.7% to 1.2 and 0.1%, respectively. These finding indicates that the high demand of wood for cooking will continue to linger among the households. In view of the above, fuel wood accounted for major part of the fuel sources for cooking in the three local governments. As more and more households depend on the use of fuel wood as a source of fuel, the demand for its exploitation has continued to increase. As a result, fuel-wood exploitation has thus gone beyond mere gathering of dead wood to deliberate and indiscriminate cutting of live trees. The disturbing aspect of fuel-wood extraction is that it can hardly be replaced. Therefore, utilization of fuel-wood in these local government areas will certainly contribute greatly to desert encroachment, and consequently has implications on the climate change and other ecological problems. Hence, the rate of rising exploitation of fuel-wood calls for serious and urgent concern at national and local levels.

Conflict of Interests

The author(s) have not declared any conflict of interests.

REFERENCES

- Ayotebi O (2000). Overview of environmental problems in Nigeria. National Centre for Economic Management and Administration (NCEMA) Paper presented at the Conference on Environment and Sustainable Development: Ibadan, 17-18 August.
- Abebaw DA (2007). Household determinants of fuelwood choice in urban Ethiopia: a case study of Jimma town. *J. Dev. Areas.* 41(1):117-126.
- Bailey NTJ (1964). *The Elements of Stochastic Processes.* Wiley, New York, pp. 15-35.
- Burley TA, O'sullivan G (1986). *Operation Research.* Macmillan Press Ltd, London. P. 178.
- Cox DR, Isham V (1980). *Point.* Chapman & Hill, London: pp. 54-55.
- Danbaba A, Isah GA (2002). Projection of Soft Drinks Consumption in Sokoto State. An Application of Markov Chain Model. *Nig. J. Basic. Appl. Sci.* 11:73-79.
- Elwood SB, James SD (1978). *Essentials of Management Science/Operations Research.* John Wiley & Sons Inc. USA: pp. 173-193.
- Hsu HP (1997). *Theory and problems of probability, random variables, and random processes.* Schaum's Outline Series, McGraw Hill New York: pp. 161-172.
- Kannan D, Lakshmikanthan V (2002). *Handbook of Stochastic Analysis and Applications.* Marcel Daker Inc. New York: pp. 4-11. <http://dx.doi.org/10.1081/SAP-120014691>
- McDonnel J, Govarde AJ, Rutten FH, Vermeiden JPW (2002). Multivariate Markov chain analysis of the probability of pregnancy in infertile couples undergoing assisted reproduction. *Hum. Reprod.* 17(1):103-106. <http://dx.doi.org/10.1093/humrep/17.1.103>
- Meredith J (1976). Program evaluation techniques in the Health Services. *Am. J. Pub. Health* 66(11):1069-1073. <http://dx.doi.org/10.2105/AJPH.66.11.1069>, PMID:824961 PMCID:PMC1653491
- National Bureau of Statistics, (2012). *Social Statistics in Nigeria,* <http://www.nigerianstat.gov.ng> accessed 12 February 2013. 11:25 A.M.
- Norris JR (1997). *Markov Chains.* Cambridge University Press U.K: pp. 40-47. <http://dx.doi.org/10.1017/CBO9780511810633>
- Richard IL, Charles AK (1975). *Quantitative Approaches to Management.* McGraw-Hill, New York, pp. 436-459.
- Ross SM (2007). *Introduction to Probability Models 9th Edition,* Academic Press Elsevier. London: pp. 185-280. PMID:17396482
- Schuss Z (2010). *Theory and Applications of Stochastic Processes, an Analytical Approach.* Springer, New York. P. 207.
- Sonnenberg FA, Beck MJ (1993). *Markov Models in Medical Decision Making: A Practical Guide.* Medical Decision Making, Hanley and Belfus, Inc. Philadelphia, PA, pp. 323-329. <http://dx.doi.org/10.1177/0272989X9301300409>
- Sung M, Erkanli A, Angold A, Castello EJ (2004). Effects of age at first substance use and psychiatric co morbidity on the development of substance use disorders. *Drug and Alcohol Dependence* 75:287-299. <http://dx.doi.org/10.1016/j.drugalcdep.2004.03.013>, PMID:15283950
- Sung M, Soyer R, Nhan N (2006). Bayesian Analysis of Nonhomogeneous Markov Chains: Application to Mental Health Data. <http://www.gwu.edu>. Accessed 12 October 2013. 10:32 P.M.
- Thierauf RJ, Klekamp RC (1975). *Decision Making Through Operations Research,* 2nd edition John Wiley & Sons Inc. New York, P. 283.
- Tijms HC (2003). *A First Course in Stochastic Models.* John Wiley & Sons Ltd. The Atrium West Sussex, England: 81-119. <http://dx.doi.org/10.1002/047001363X>
- Welton NJ, Ades AE (2005). Estimation of Markov chain transition probabilities and rates from fully and partially observed data: uncertainty propagation, evidence synthesis and model calibration. *Medical Decision Making.* 25(633):633-645. <http://dx.doi.org/10.1177/0272989X05282637> PMID:16282214
- Williams M (2003). *Deforesting the earth from prehistory to Global Crisis.* American Forests. University of Chicago Press.

Full Length Research Paper

Studies on zinc oxide thin films by chemical spray pyrolysis technique

Prabakaran Kandasamy* and Amalraj Lourdasamy

Research Center in Physics, VHNSN College, Virudhunagar – 626001, Tamilnadu, India.

Received date 25 April, 2014; Accepted 28 May, 2014

Zinc oxide (ZnO) thin films were deposited by chemical spray pyrolysis (CSP) technique using zinc acetate dihydrate solutions on microscopic glass substrates by varying the precursor concentration. The prepared films were characterized structurally and optically, using the powder X-ray diffraction (XRD) and UV analysis and Photoluminescence analysis. Crystallographic properties were analyzed through powder XRD. The XRD patterns shows a hexagonal structure with c-axis orientation (0 0 2) on self texturing phenomenon. Optical transmittance properties of the optimized ZnO thin films were investigated by using UV-Vis spectroscopy. The optical studies predicated a maximum transmittance in the range of above 70% with direct band gap values in the range of 2.9 to 3.2eV for the zinc oxide thin films. Under excitation of 300 nm radiations, sharp deep level emission peak at 2.506 eV dominates the photoluminescence spectra with weak deep level and near band edge emission peak at 3.026 and 3.427 eV respectively.

Key words: Transparent conducting oxide (TCO), Zinc Oxide thin film, CSP technique, X-ray diffraction (XRD), UV-Vis, Photoluminescence.

INTRODUCTION

Metal oxide semiconductor thin films have been widely researched and have received considerable attention in recent years due to their optical and electrical properties. Because they are good candidates for transparent conducting oxide (TCO) films (Hongxia et al., 2005). Zinc oxide is (ZnO) a wide direct band gap (~3.37eV at T=300 K) semiconductor (II-VI) which has been widely investigated in the past years for more literature. ZnO also has a high exciton binding energy of 60 meV which is higher than the values of other widely used wide band gap materials, such as ZnSe (20 meV) and GaN (21 meV). The large exciton binding energy can ensure

efficient excitonic emission at room temperature (Zahedi and Dariani, 2012). Exciton provides a sensitive indicator of material quality. Photoluminescence (PL) is very sensitive to the quality of crystal structure and to the presence of defects (Sagar et al., 2007). ZnO has a large transparency in the visible region, high natural abundance, absence of toxicity, low cost compared to other oxide materials such as SnO₂, In₂O₃, TiO₂ (Mahalingam et al., 2003; Gaikwad et al., 2012). In generally, thin films are depends not only on the morphology of the sample, but also on the deposition parameters, thickness of the sample and grain sizes

*Corresponding author. E-mail: karan_phy07@yahoo.com

Author(s) agree that this article remain permanently open access under the terms of the [Creative Commons Attribution License 4.0 International License](https://creativecommons.org/licenses/by/4.0/)

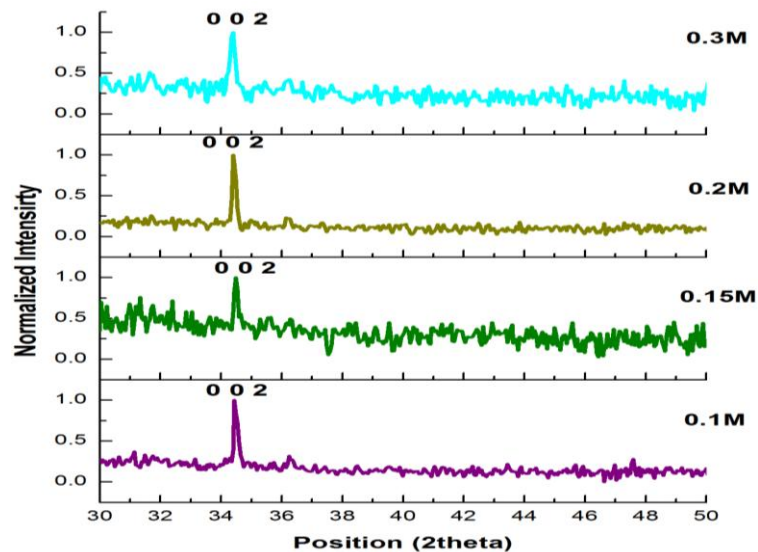


Figure 1. X-Ray pattern of ZnO thin film at (a) 0.1 M, (b) 0.15 M, (c) 0.2 M, (d) 0.3 M.

(Godbole et al., 2011). In recent years, the ZnO based films has potential applications in the field of electronic devices such as gas sensors, solar cells, optoelectronics, thin film transistors (Kuo et al., 2006; Chu et al., 2009; Van Heerden et al., 1997; Joseph et al., 1999a; Wei et al., 2007; Mani et al., 2006). Many deposition techniques have been used to prepared zinc oxide thin films in order to improve their properties such as, chemical bath deposition (CBD) (Kathirvel et al., 2009) Sol-gel spin coating (Natsume and Sakata, 2000), metal organic chemical vapour deposition (Wang et al., 2004), RF-magnetron sputtering (Shiyi et al., 2009), spray pyrolysis (Achour et al., 2007; Joseph et al., 1999a; Yoon and Cho, 2000; Ayouchi et al., 2003). Compared to the others, the spray technique has many advantages: it is easy, inexpensive, safety and the low cost of the apparatus and the raw materials, no sophisticated instrument such as vacuum systems etc., large area coating of thin film and well adopted for mass fabrication (Manouni et al., 2006; Gencyilmaz et al., 2013; Saleem et al., 2012). Furthermore, the optical, structural properties of thin films can be easily controlled by the quantity of sprayed solution in this technique. In general, the films produced with this technique are polycrystalline, stable, adherent, and hard. Spray pyrolysis has been developed as a powerful tool for preparation on various kinds of technological materials such as metals, metal oxides, superconducting materials, and nanophase materials (Saleem et al., 2012). In the present work, we report the thickness on mainly structural and optical properties involved during the effect of precursor concentration on the X-ray diffraction (XRD), UV-Visble and photoluminescence behavior of ZnO thin films deposited by chemical spray pyrolysis technique.

EXPERIMENTAL PROCEDURES

The zinc oxide films were deposited on microscopic glass substrates (Thickness 1.35 mm) at a constant temperature of 380°C with an accuracy of $\pm 5^\circ\text{C}$ by a chemical spray pyrolysis technique at various precursor concentrations. A solution of 0.1, 0.15, 0.2 and 0.3 M zinc acetate dihydrate was used as a precursor prepared by dissolving in mixture of deposited water and isopropyl alcohol (1:3) volume ratio. The nozzle was at a distance of 24 cm from the substrate during deposition. The solution flow rate was held 4 ± 0.5 ml/min. Compressed air was used as the carrier gas. The pressure of the carrier gas should be 0.7 Kg/cm². The deposited films were allowed to cool down to room temperature.

The structure of the films were examined by using XPERT – PRO' X-Ray diffractometer with CuK α_1 radiation ($\lambda=1.54056 \text{ \AA}$). The thickness of the films was determined by stylus profilometer. The optical transmission spectroscopic measurements of the zinc oxide thin films were carried out at room temperature using SHIMADZU - 1800 Double beam Spectrophotometer in the wavelength range between 300 – 700 nm. VARAIN CARRY ECLIPSE Spectrophotometer excited with 300 nm wavelength from a xenon lamp was used to record photoluminescence spectra of the films.

RESULTS AND DISCUSSION

XRD analysis

X-Ray diffractograms of films prepared at different precursor concentration (0.1 to 0.3 M) was shown on Figure 1. All the diffractograms of the prepared films clean indicate the polycrystalline nature of zinc oxide films with prominent diffraction peak from crystal plane (0 0 2) on self-texturing phenomenon (Chougule et al., 2010) had also obtained a single peak in their XRD pattern by Sol-gel spin coating method with (0 0 2)

Table 1. XRD data of ZnO thin film.

Precursor concentration (M)	Observed values		Thickness (nm)	Grain size (nm) (k=0.9)
	2θ (deg)	lattice constant (c) Å°		
0.1	34.4582	5.2013	103	70.12
0.15	34.4779	5.1986	110	46.23
0.2	34.4005	5.2098	158	84.38
0.3	34.3203	5.2216	145	11.55

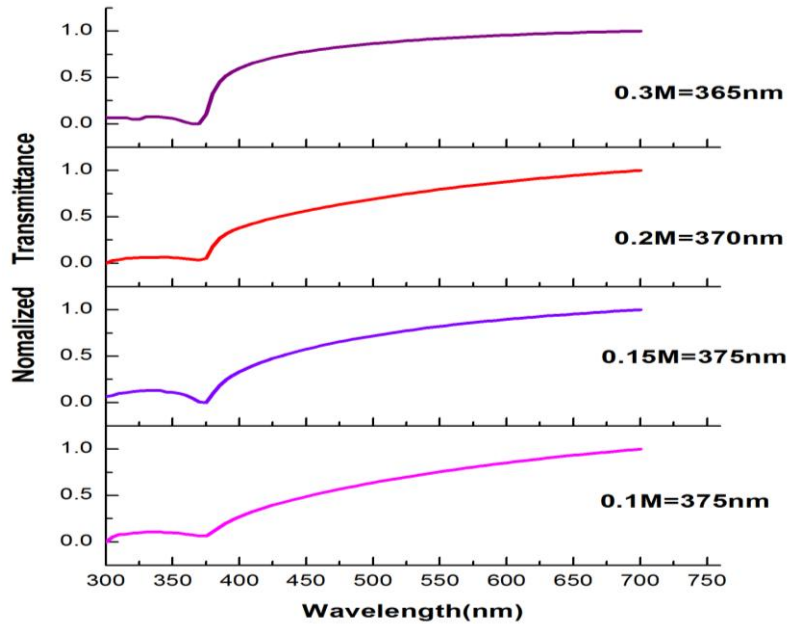


Figure 2. Transmittance spectrum of ZnO thin film.

plane reflection. The deposition of precursor concentration increased without the appearance of any new reflections. Thus no other phases were formed. The phase identification revealed that only hexagonal crystal system based zinc oxide (JCPDS File No.75-1526, 80-0075, 80-0074) was conformed. The lattice constant “C” was calculated by using the following equation:

$$\frac{1}{d^2} = \frac{4}{3} \left[\frac{h^2 + hk + k^2}{a^2} \right] + \frac{L^2}{C^2} \tag{1}$$

The calculated values of the lattice constant (c) are found to be close to those of the Joint Committee on Powder Diffraction Standard (JCPDS) data reported for zinc oxide sample. The average grain size was measured using Debye-Scherrer’s formula (Cullity, 1978):

$$Grainsize(D) = \frac{0.9 * \lambda}{\beta \cos \theta} \text{ (nm)} \tag{2}$$

Where λ is the wavelength of Cu Kα1 radiation (1.54056 Å°), β is the FWHM value. The variation of film thickness, grain size, lattice constant (c), two theta with precursor concentration are shown in Table 1.

Optical properties

The transmittance spectrum of ZnO thin films in the wavelength range 300 - 800 nm are shown in the Figure 2. Optical properties of the zinc oxide thin films were studied with the help of transmission spectrum in the UV-visible region. Figure 2 shows the transmittance spectrum of zinc oxide films deposited at different precursor concentration recorded in the range 300 to 700 nm. The spectrum shows a maximum transparency of >70% in the visible region. Sharp ultraviolet absorption edges at λ=375 nm are observed with the absorption edge being shifted to shorter wavelength at higher concentration. It can be clearly seen the blue shift in band edge in Figure 3. The optical absorption coefficient can be calculated

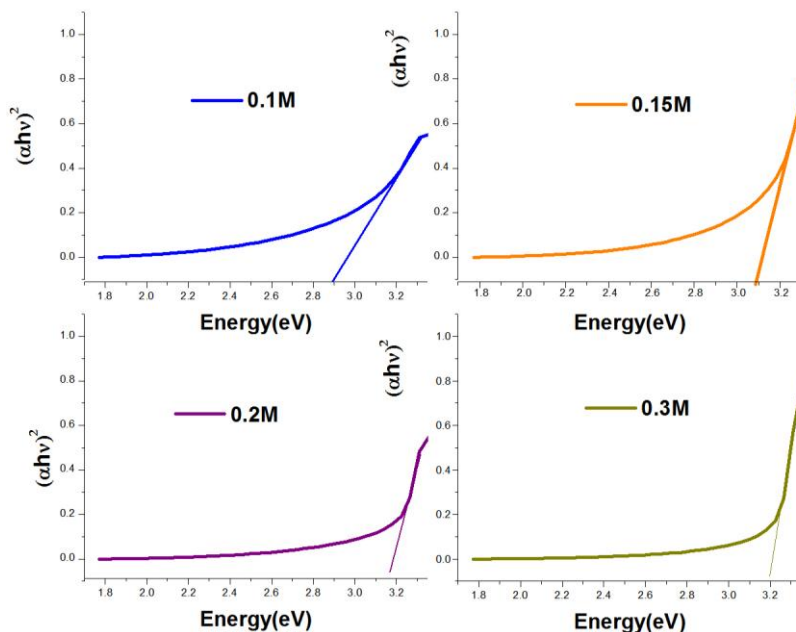


Figure 3. Variation of $(\alpha hv)^2$ versus $h\nu$ of the zinc oxide thin film.

Table 2. Transmittance at maximum, 550 nm and direct band gap for different precursor concentration.

Precursor concentration (M)	Direct band gap (eV)	Transmittance (%) T_{max}	Transmittance (%) T_{550nm}
0.1	2.9	73.345	61.88
0.15	3.1	88.603	79.93
0.2	3.18	74.602	61.51
0.3	3.20	87.372	82.78

using the Lambert law relation

$$\alpha = t * \ln\left(\frac{1}{T}\right) \quad (3)$$

where t is the thickness of the film and T the transmittance. The relation between absorption coefficient and incident photon energy can be written as:

$$(\alpha hv) = A(hv - E_g)^{\frac{1}{2}} \quad (4)$$

Where A is a constant, E is the band gap of the material and h is the planks constant. In the present case, the plot of $(\alpha hv)^2$ versus $h\nu$, indicates the direct band gap nature of the films. By extrapolating the linear portion of the curve onto the X-axis the energy band gap of the films is determined. The transmittance at maximum 700 and 550

nm, and direct band gap for different precursor concentration was shown in Table 2. Thus on increase in band gap was observed, when the concentration was changed from 0.1 to 0.3 M. This may be due to the hexagonal phase. The effect of bandgap widening is attributed primarily to the Moss-Burstein shift in semiconductors. The bandgap changes found is in good agreement with reported values 3.14 to 3.26 eV by the same spray pyrolysis technique (Joseph et al., 1999b).

The photoluminescence property of film has a close relation with the crystalline, because the density of defects in the film reduces with an improvement of the crystallinity. Room temperature PL emission spectrum for all the samples was measured in the wavelength range of 310 to 550 nm at the excitation wavelength of 300 nm. PL spectra of the zinc oxide thin films deposited on glass substrates at various precursor concentrations are shown in Figure 4. The zinc oxide emission is generally classified into two categories one is the UV emission of all zinc oxide thin films at 3.427 eV and the other is the

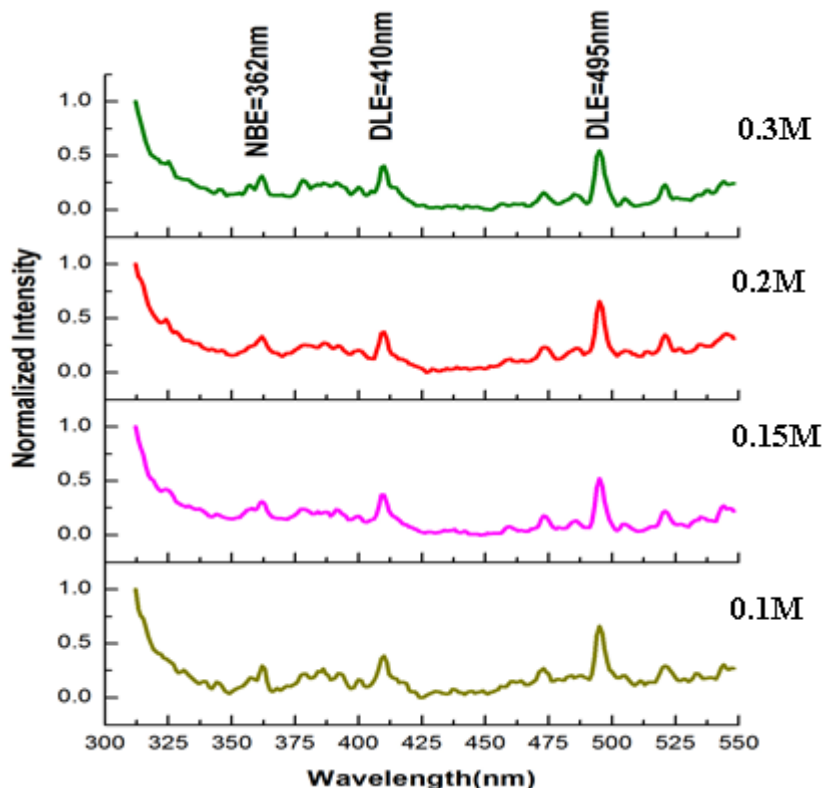


Figure 4. Comparison of the variation of peak intensity with different concentrations.

deep level (DL) emission related to the defect emission in the visible range. In the deep level emission, two emission peaks at 3.026 and 2.506 eV appear in the PL spectra shows a strong blue emission band (Gao et al., 2004) around 2.506 eV in all samples. By comparing the results from absorption spectra and PL spectra, pronounced exciton absorption peak in the UV spectra located at around 3.4 eV is assigned to the exciton effect in ZnO. It is clear that the above results exists a stokes shift between the PL spectra and the absorption spectra. The stokes shift is related to many effects such as electron–phonon coupling, lattice distortions, interface defects and point defects that may cause the blue shift of emission line from absorption edge (Sagar et al., 2007). In the case of blue shift, the filling of the conduction band by electrons will generally result in the NBE emission. The stokes shift were calculating the following equation:

$$\Delta E = E_{Abs} - E_{PL} \quad (5)$$

The stokes shifts were calculated to be much larger value respectively for increase in the molar concentration for ZnO thin films. The crystalline quality of ZnO film grain size has a larger distribution leading to PL band (Shan et al., 2006).

Conclusion

Zinc oxide thin film was deposited on the glass substrate by chemical spray pyrolysis technique. The XRD studies show that, films prepared are in nanocrystalline range. Polycrystalline nature of zinc oxide films and lattice parameter (C) has been determined which agree with the standard data. From the X-ray diffraction analysis 0.1, 0.15, 0.2 and 0.3 M films show hexagonal structure along with *c*-axis oriented (0 0 2) plane. Optical transmittance properties of the optimized ZnO thin films were investigated by using UV-Vis spectroscopy. The transmittance of above 70% in the visible region has been observed for precursor concentration and increase the concentration caused by the band gap to become broader. An intensive blue luminescence peak around 495 nm is observed at room temperature.

Conflict of Interests

The author(s) have not declared any conflict of interests.

ACKNOWLEDGEMENTS

The authors would like to thank Dr. Sanjeeviraja

Chinnappanadar, Department of Physics, Alagappa University, Karaikudi and Department of Botany, V.H.N.S.N.College, Virudhunagar for this valuable help to obtaining their characterization of work.

REFERENCES

- Achour ZB, Ktari T, Ouertani B, Touayar O, Bessais B, Brahim JB (2007). Effect of doping level and spray time on zinc oxide thin films produced by spray pyrolysis for transparent electrodes applications. *Sens. Actuators, A* 134(2):447-451. <http://dx.doi.org/10.1016/j.sna.2006.05.001>
- Ayouchi R, Leinen D, Martin F, Gabas M, Dalchiale E, Ramos-Barrado JR (2003). Preparation and characterization of transparent ZnO thin films obtained by spray pyrolysis. *Thin Solid Films*, 426(1):68-77. [http://dx.doi.org/10.1016/S0040-6090\(02\)01331-7](http://dx.doi.org/10.1016/S0040-6090(02)01331-7)
- Chu D, Hamada T, Kato K, Masuda Y (2009). Growth and electrical properties of ZnO films prepared by chemical bath deposition method. *Phys. Status Solid A*, 206(4):718-723. <http://dx.doi.org/10.1002/pssa.200824495>
- Gaikwad RS, Patil GR, Shelar MB, Pawar BN, Mane RS, Han SH, Joo OS (2012). Nanocrystalline ZnO films deposited by spray pyrolysis: Effect of gas flow rate. *Int. J. Self Propag. High Temp. Synth.* 21(3):178-182. <http://dx.doi.org/10.3103/S106138621203003X>
- Gencyilmaz O, Atay F, Yavuz I (2013). Preparation and Characterization of Transparent, Conductive ZnO Thin Film for Photovoltaic Solar Cells. *J. Selcuk Univer. Nat. Appl. Sci.* pp. 752-759.
- Godbole B, Badera N, Shrivastava S, Jain D, Ganesan V (2011). Growth mechanism of ZnO films deposited by spray pyrolysis technique. *Mater. Sci. Appl.* 2:643. <http://dx.doi.org/10.4236/msa.2011.26088>
- Hongxia L, Jiyang W, Hang L, Huajin Z, Xia L (2005). Zinc oxide films prepared by sol-gel method. *J. Cryst. Growth*, 275:e943-e946. <http://dx.doi.org/10.1016/j.jcrysgro.2004.11.098>
- Joseph B, Gopchandran KG, Manoj PK, Peter K, Thomas PV, Vaidyan VK (1999b). Optical and electrical properties of zinc oxide films prepared by spray pyrolysis. *Bull. Mater. Sci.* 5:921-926. <http://dx.doi.org/10.1007/BF02745554>
- Joseph B, Gopchandran KG, Thomas PV, Koshy P, Vaidyan VK (1999a). A study on the chemical spray deposition of zinc oxide thin films and their structural and electrical properties. *Mater. Chem. Phys.* 58(1):71-77. [http://dx.doi.org/10.1016/S0254-0584\(98\)00257-0](http://dx.doi.org/10.1016/S0254-0584(98)00257-0)
- Kathirvel P, Manoharan D, Mohan SM, Kumar S (2009). Spectral investigations of chemical bath deposited zinc oxide thin films ammonia gas sensor. *J. Optoelectr. Biomed. Mater.* 1(1):25-33.
- Kuo SY, Chen WC, Lai FI, Cheng CP, Kuo HC, Wang SC, Hsieh WF (2006). Effects of doping concentration and annealing temperature on properties of highly-oriented Al-doped ZnO films. *J. Cryst. Growth*, 287(1):78-84. <http://dx.doi.org/10.1016/j.jcrysgro.2005.10.047>
- Mahalingam T, John VS, Sebastian PJ (2003). Growth and characterization of electrosynthesised zinc oxide thin films. *Mater. Res. Bull.* 38(2):269-277. [http://dx.doi.org/10.1016/S0025-5408\(02\)01036-X](http://dx.doi.org/10.1016/S0025-5408(02)01036-X)
- Mani B, Manjon FJ, Mollar M, Cembrero J, Gomez R (2006). Photoluminescence of thermal-annealed nanocolumnar ZnO thin films grown by electrodeposition. *Appl. Surf. Sci.* 252 2826-2831. <http://dx.doi.org/10.1016/j.apsusc.2005.04.024>
- Manouni AE, Manjón FJ, Mollar M, Marí B, Gómez R, López MC, Ramos-Barrado JR (2006). Effect of aluminium doping on zinc oxide thin films grown by spray pyrolysis. *Superlattices Microstruct.* 39(1):185-192. <http://dx.doi.org/10.1016/j.spmi.2005.08.041>
- Natsume Y, Sakata H (2000). Zinc oxide films prepared by sol-gel spin-coating. *Thin solid films*, 372(1):30-36. [http://dx.doi.org/10.1016/S0040-6090\(00\)01056-7](http://dx.doi.org/10.1016/S0040-6090(00)01056-7)
- Shiyi Z, Yuying X, Min G (2009). Magnetic properties of ZnO: Cu thin films prepared by RF magnetron sputtering. *J. Semicond.* 30(5): 052004. <http://dx.doi.org/10.1088/1674-4926/30/5/052004>
- Van Heerden JL, Swanepoel R (1997). XRD analysis of ZnO thin films prepared by spray pyrolysis. *Thin Solid Films*, 299(1):72-77. [http://dx.doi.org/10.1016/S0040-6090\(96\)09281-4](http://dx.doi.org/10.1016/S0040-6090(96)09281-4)
- Wang J, Du G, Zhang Y, Zhao B, Yang X, Liu D (2004). Luminescence properties of ZnO films annealed in growth ambient and oxygen. *J. Cryst. Growth*, 263(1):269-272. <http://dx.doi.org/10.1016/j.jcrysgro.2003.11.059>
- Wei XQ, Zhang ZG, Liu M, Chen CS, Sun G, Xue GS, Zhuang HZ, Man BY (2007). Annealing effect on the microstructure and photoluminescence of ZnO thin films. *Mater. Chem. Phys.* 101(2):285-290. <http://dx.doi.org/10.1016/j.matchemphys.2006.05.005>
- Yoon KH, Cho JY (2000). Photoluminescence characteristics of zinc oxide thin films prepared by spray pyrolysis technique. *Mater. Res. Bull.* 35(1):39-46. [http://dx.doi.org/10.1016/S0025-5408\(00\)00183-5](http://dx.doi.org/10.1016/S0025-5408(00)00183-5)
- Zahedi F, Dariani RS (2012). Effect of precursor concentration on structural and optical properties of ZnO microrods by spray pyrolysis. *Thin Solid Films*, 520(6):2132-2135. <http://dx.doi.org/10.1016/j.tsf.2011.09.006>
- Saleem M, Fang L, Wakeel A, Rashad M, Kong CY (2012). Simple Preparation and Characterization of Nano-Crystalline Zinc Oxide Thin Films by Sol-Gel Method on Glass Substrate. *World J. Condens. Matter Phys.* 2:10-15. <http://dx.doi.org/10.4236/wjcmp.2012.21002>
- Chougule MA, Patil SL, Pawar SG, Patil VB (2010). Transparent and conductive ZnO: Al thin films prepared by sol-gel process. *Archives Phys. Res.* 1(1):100-107.
- Cullity BD (1978) *Elements of X-ray Diffraction*, Addison Wesley, Reading, M.A, P. 102.
- Gao XD, Li XM, Yu WD (2004). Preparation, structure and ultraviolet photoluminescence of ZnO films by a novel chemical method. *J. Solid State Chem* 177(10):3830-3834. <http://dx.doi.org/10.1016/j.jssc.2004.07.030>
- Sagar P, Shishodia PK, Mehra RM, Okada H, Wakahara A, Yoshida A (2007). Photoluminescence and absorption in sol-gel-derived ZnO films. *J. Lumin.* 126(2):800-806. <http://dx.doi.org/10.1016/j.jlumin.2006.12.003>
- Shan FK, Liu GX, Lee WJ, Shin BC (2006). Stokes shift, blue shift and red shift of ZnO-based thin films deposited by pulsed-laser deposition. *J. crystal growth*, 291(2):328-333. <http://dx.doi.org/10.1016/j.jcrysgro.2006.03.036>

Full Length Research Paper

Kinematics of the human hand applied to the design of prosthesis

Luis Antonio Aguilar-Pérez¹, Christopher René Torres-San Miguel^{1*}, Guillermo Urriolagoitia-Sosa¹, Luis Martínez-Sáez², José Alfredo Leal-Naranjo¹, Beatriz Romero-Ángeles³ and Guillermo Urriolagoitia-Calderón¹

¹Instituto Politécnico Nacional, Escuela Superior de Ingeniería Mecánica y Eléctrica; Unidad Profesional Zacatenco, Av. Instituto Politécnico Nacional s/n, Col. Lindavista, Delegación. Gustavo A. Madero, Distrito Federal, C.P. 07738, México.

²Instituto Universitario de Investigación del Automóvil, Industriales, Universidad Politécnica de Madrid. Carretera de Valencia, km.7. Madrid, España. CP. 28031, México.

³Instituto Politécnico Nacional, Escuela Superior de Ingeniería Mecánica y Eléctrica, Unidad Profesional Azcapotzalco, Av. De las Granjas No. 682, Col. Santa Catarina. Del. Azcapotzalco, Distrito Federal C.P. 02250 México.

Received 31 October, 2013; Accepted 12 May, 2014

This work shows the application of a mechanism of four bars synthesized function used in the development of a prosthetic device with an underactuated movement, for its application in people with a mutilation level close to the distal dislocation of the wrist. A methodology is exposed for this, from which the procedure for obtaining the trajectory of the four bars mechanism through the function synthesis, which was formulated upon two mathematic models expressed in terms of anthropometric values and ranges of movement for the index and thumb, respectively. As a result of the synthesis of these mechanisms a hand prosthesis prototype was obtained, which counts with seven degrees of liberty separately from each other, which allows to develop punctual and cylindrical holdings, with the purpose of applying this prototype to the subsequent study of grip patterns and interpretation of myoelectric signals that allow to determine an easier to interpret mechanism of control that permits to generate dynamic grips instead of static average grips.

Key words: Computer Aided Design (CAD), Biomechanics, synthesis of mechanisms.

INTRODUCTION

The purpose of generating a grip movement with the hand is to achieve the thumb, along with any of the other fingers, wraps the object of interest within the workload of the entire hand. A precise simulation of this behavior represents such a high degree of complexity due to all

implicit variables during the custom scan features of the human being (Belter and Dollar, 2011). Therefore, it is important to mention that the design process of prototypes must satisfy the best possible way, the personal characteristics of each patient which are defined

*Corresponding author. E-mail: ctorress@ipn.mx

Author(s) agree that this article remain permanently open access under the terms of the [Creative Commons Attribution License 4.0 International License](https://creativecommons.org/licenses/by/4.0/)

under three general points of view: the description of anthropometric and morphological characteristics of the hand (Zollo et al., 2007; Naik and Kumar, 2010), the work device capabilities (Kutz, 2003), and the control exerted by the person itself.

The opposition movement is the most important, being described by Kapandji and Lacomba (2006) as a set of three consecutive moves: first the preemption of the full osteoarticular column, followed by its flexion to suit the action to perform, and ending with the complete opposition of the thumb on the hand. In Santos (Barrientos et al., 2007) analysis of the five axes of motion that make up the complete thumb osteoarticular column was proposed, finding that the major joints were the carpal metacarpal joint (CMC) and the metacarpophalangeal (MCP), which is why the authors conclude that the study of these two joints is impossible to perform separately, so Kapandji and Lacomba (2006) established that the movements of the thumb may be explained with only three motion axes, joining the CMC and MCP joints in a single joint, and neglecting the offset of the multangular-metacarpal joint (TMC). In Light (Cimadevilla and Herrera, 2006) it was mentioned that the main importance of flexing moves is due to the fact that through these, it is possible to "wrap" the object with the fingers, while the abduction-adduction allows, in a certain way, to "guide" the finger so that it can stably hold the object.

Furthermore, Barrientos et al. (2007) mentioned that a singular configuration is acquired due to the alignment of two or more phalanges able to reach the same point, but using different angular positions, so that in the work reported by Cimadevilla and Herrera (2006) and Hernández and Montoya (2007), it was shown that there was a slight dependence between the movement of the last joints from the fingers II and III, but this became larger between fingers IV and V. Anatomically fingers II to V have the same type of metacarpophalangeal joint (MCP), which is a condylar type, allowing to generate flexion and extension as well as abduction and adduction movement, but since the range of motion of the latter is too small, between 10° and 15° , compared with the first type of movement is a range of about -20° to 110° , generally this type of movement is omitted in the prosthetic design.

Due to the wide range of objects that people manipulate daily, usually the types of grips are divided into two, depending on the action seeking to perform, either manipulate (dynamic grip) or hold (static grip) any element by a previously established position for an undefined time. According to the results shown by Vergara et al. (2012) it was found that the main types of static grip used in daily life were the cylindrical type (determined for force grips) and precise (determined for precision grips), while eating was the activity with a longer allotted time as well as the tasks associated with this, giving it an average of 1.604 h a day, followed by leisure tasks (1.086 h/day) and grooming (0.76 h/day).

On the other hand, the index and middle fingers of a human hand exert a maximum average force of 50 to 60 N, while the ring and little finger exert a maximum force of 25 to 35 N average as reported in Gregory (2002). A study by Alcalde et al. (2006) in Spain, shows that the thumb can exert a maximum average force of 91 to 101.6 N, concluding that when the force is exerted by a finger individually, the range of applied force is greater than the one that would be determine if this were other fingers participating during grip (Table 4) (Li et al., 1998).

The literature reports that the statically interaction with objects takes two forms; first if the item is held for a long time and its size is medium or even small, then a precision grip is required (Feix et al., 2009) performed between the index finger and thumb (although it also interacts with the medium finger), on the other hand, if it's necessary to hold a heavy object for a short time or if its size is medium or even large, a grip with force will be done by the whole hand, being named this as grip power grip (Cipriani et al., 2006).

There is a third type of movement that is performed from the junction between the two above, but due to the redundancy of positions that should be adopted to perform this grip, the study of this would be repetitive in terms of the positions a hand adopts during gripping. Because of this wide variability of objects, it is difficult to determine a specific design under which the special characteristics of each task is defined, combined with, due to amputation suffered by the patient, the control exercised by the person on the prosthesis, commonly is used to take positions of the remaining member, which will be performed by the device so that these can be translated into a static position defined as grip (Feix et al., 2009). Thus, this paper proposes the development of a methodology for sizing four-bar mechanisms, which are adaptable to custom prosthetic hands design at the level range of motion and specific anthropometric dimensions of the persons hand.

MATERIALS AND METHODS

The methodology presented in this paper consists of the kinematic analysis of the open chain representing the fingers, performed from the procedure described by Denavit and Hartenberg following the convention of signs and symbols given by Craig (2006); Lewis et al., (2004) and Shigley and Uicker (2001) from where the equations that describe the position of the fingertip are obtained, which can be adapted to a mathematical function that is used as a movement pattern for the synthesis of the mechanism function and are solved by Shigley and Uicker (2001) and Montúfar et al. (2009), method, obtaining as a result the dimensions of two types of mechanisms, one for the thumb and one for the index finger, to be finally adapted to the dimensions of a physical prototype, which will be generated by the CAD/CAE/CAM methodology described by Costa-de-Morais (2003) and Candal (2005) which is adapted to this case study.

Miralles and Puig (2000) and Portilla et al. (2010) proposed various ranges of values used to define the kinematics of the hand, Table 1 summarizes several sources regarding to the anthropometric measurements of the index finger, which are referenced in the following schematic figure from the index finger.

Table 1. Measures of the forefinger offered by different authors.

Joint	Kind of movements	Forefinger			
		Miralles and Puig (2000)	Velázquez Sánchez (2008)	Portilla et al. (2010b)	Aguilar (2013)
MCP	Extension	22°	30°
	Flexion	86°	98°	83°	84°
	Length	45 mm	43 mm	43 mm	45 mm
IPP	Extension	7°	15°
	Flexion	102°	115°	105°	104°
	Length	22 mm	26 mm	26 mm	22 mm
IPD	Extension	8°	3°
	Flexion	72°	78°	78°	78°
	Length	27 mm	23 mm	16 mm	25 mm

Table 2. Measures of the thumb offered by different authors.

Joint	Kind of movement	Thumb		
		Chang and Matsuoka (2006)	Deshpande et al. (2013)	Aguilar (2013)
TM	F-E	53°	40° - 40°.	35°, 40°.
	A-A	42°	40° - 40°.	40°, 10°.
	Length	52.9 mm	43.1 mm	46 mm
	F-E	70°	60° - 60°.	70°, 40°.
MCP	A-A	30°	15° -15°.	50° - 40°.
	Length	40.3 mm	36.5 mm	34.5 mm
	F-E	95°-100°	20° - 80°	60° - 40°
	A-A	---	---	---
IP	Length	30.7 mm	20 mm	30 mm

Due to the previously described anatomical and morphological similarity between the finger II (index) and fingers III to V, the study and application of the methodology proposed herein will be omitted. Likewise, in Table 2, the anthropometric values and ranges of motion of the thumb reported by several authors are summarized, these were measured from the reference shown in Figure 2, being the result of simplified joint raised previously. Using the values reported in the last column of Tables 1 and 2 -beside from the use of the methodology described by Barrientos et al. (2007) from

Figures 1 and 2, Equations (1) to (5) are obtained, which describe the position of the fingertips from the direct kinematics of the open string that represent them.

$$posx_{ff} = l_1 \cos(q_1) + l_2 \cos(q_1 + q_2) + l_3 \cos(q_1 + q_2 + q_3) \tag{1}$$

$$posy_{ff} = l_1 \sin(q_1) + l_2 \sin(q_1 + q_2) + l_3 \sin(q_1 + q_2 + q_3) \tag{2}$$

$$posx_{th} = l_1 c_{q_1} + l_2 (c_{(q_1+q_2)} c_{q_1} - s_{(q_1+q_2)} c_{\alpha_1} s_{q_1}) - l_3 a (c_{(\alpha_1+\alpha_2)} s_{(q_1+q_2)} c_{q_1} - s_{(\alpha_1+\alpha_2)} s_{\alpha_1} c_{q_1} + c_{(\alpha_1+\alpha_2)} c_{(q_1+q_2)} c_{\alpha_1} s_{q_1}) + l_3 b (c_{(q_1+q_2)} c_{q_1} - s_{(q_1+q_2)} c_{\alpha_1} s_{q_1}) \tag{3}$$

$$posy_{th} = l_1 s_{q_1} + l_2 (c_{(q_1+q_2)} s_{q_1} + s_{(q_1+q_2)} c_{\alpha_1} c_{q_1}) - l_3 a (c_{(\alpha_1+\alpha_2)} s_{(q_1+q_2)} s_{q_1} + s_{(\alpha_1+\alpha_2)} s_{\alpha_1} c_{q_1} - c_{(\alpha_1+\alpha_2)} c_{(q_1+q_2)} c_{\alpha_1} c_{q_1}) + l_3 b (c_{(q_1+q_2)} s_{q_1} + s_{(q_1+q_2)} c_{\alpha_1} c_{q_1}) \tag{4}$$

$$posz_{th} = l_2 s_{(q_1+q_2)} s_{\alpha_1} + l_3 a (s_{(\alpha_1+\alpha_2)} c_{\alpha_1} + c_{(\alpha_1+\alpha_2)} c_{(q_1+q_2)} s_{\alpha_1}) + l_3 b (s_{(q_1+q_2)} s_{\alpha_1}) \tag{5}$$

Where;

$$a = s_{(q_1+q_2+q_3)}$$

$$b = c_{(q_1+q_2+q_3)}$$

From the above equations, the ideal workspace for both fingers shown in Figure 3a and b for the index to the thumb was plotted, so they were the visual references for the evaluation of the operating range and determining the movement pattern proposed in this research. it was mentioned before that the morphology of the

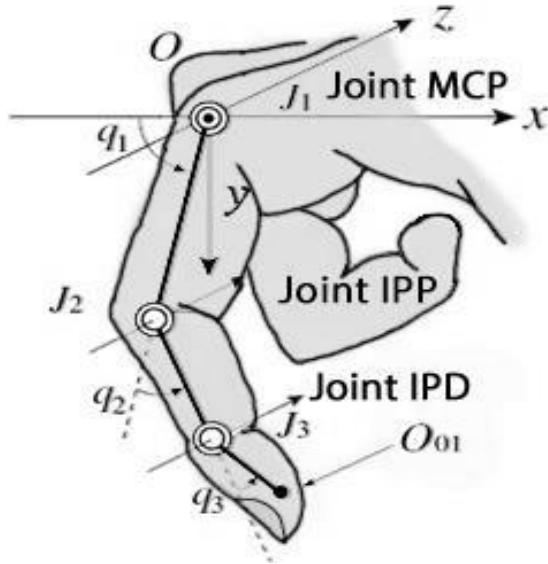


Figure 1. Links that represent the forefinger.

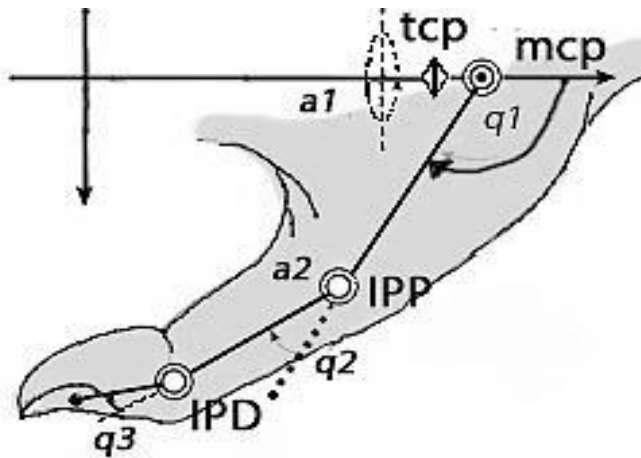


Figure 2. Links that represents the thumb.

forefinger it is dependent between phalanx, that is why the value of input like function of the previous phalanx was determine and was expressed in Equation (6), limited by the range of movements shows in Table 1 at the last column.

$$f(\theta_{1ff}) = \sin \theta_i \tag{6}$$

Thus, for the thumb an anthropometric relationship between this parameter and its mathematical relationship was established with respect to a parametric function modeled on the approximation of the workspace volume reported by Li and Tang (2007) and Zhang et al. (2005).

$$f(u, v, k) = \begin{bmatrix} x(u, v, k) \\ y(u, v, k) \\ z(u, v, k) \end{bmatrix} = \begin{bmatrix} r * \cos(u) \\ r * \sin(u) \\ v \end{bmatrix} \tag{7}$$

Whose equation is shown below was established.

$$r = f(X) = \frac{(posy2 - posy1)}{(posx2 - posx1)}(X - posx2) + posy2$$

$$v = TM_{length} + MCP_{length} + IP_{length}$$

To do the synthesis of mechanism it was necessary to establish some precision points which are result of the evaluation of Equations (6) and (7), which are in the range of values of Tables 1 and 2. That evaluation was made by using the Chebichev equation, which is shown in Equation (8).

$$x_j = \frac{1}{2}(x_0 + x_{n+1}) - \frac{1}{2}(x_{n+1} - x_0) * \cos\left(\frac{\pi(2j-1)}{2n}\right) \quad j = 1, 2, \dots, n \tag{8}$$

For the use of Equation (8), for each set of mechanisms 21 precision points were determined, plus the synthesis of the mechanism from the thumb was performed only in the XY plane, since in this plane is possible to describe the motion of flexion - extension of the thumb. The result of this evaluation was substituted in the Freudenstein equations shown by Equations (14) and (15), so that, in attempting to satisfy these values, it was necessary to solve a system of equations with 21 unknowns quantities, for which we used the Newton-Raphson method shown in Equation (16), besides being considered the procedure described by Shigley and Uicker (2001) and Montúfar et al., (2009).

$$K_2 \cos \theta_4 - K_3 \cos \theta_2 + K_1 = \cos(\theta_2 - \theta_4) \tag{14}$$

$$K_2 \cos \theta_3 - K_5 \cos \theta_2 + K_4 = \cos(\theta_2 - \theta_3) \tag{15}$$

$$X_{k+1} = X_k - \frac{f(X_k)}{J(X_k)} \tag{16}$$

Where:

$$K_1 = \frac{a_1^2 + a_4^2 + a_2^2 - a_3^2}{2 * a_2 * a_4}$$

$$K_2 = \frac{a_1}{a_2}$$

$$K_3 = \frac{a_1}{a_3}$$

$$K_4 = \frac{a_4^2 + a_2^2 + a_3^2 - a_1^2}{2 * a_2 * a_3}$$

$$K_5 = \frac{a_1}{a_3}$$

$$J = \begin{bmatrix} j_{1,1} & \dots & j_{m,n} \\ \vdots & & \vdots \\ j_{m,1} & \dots & j_{m,n} \end{bmatrix} \tag{17}$$

$$j_{1,1} = \frac{\delta F_1}{\delta X_1}; j_{1,2} = \frac{\delta F_1}{\delta X_2}; \dots; j_{1,n} = \frac{\delta F_1}{\delta X_n}$$

$$j_{m,1} = \frac{\delta F_m}{\delta X_1}; j_{m,2} = \frac{\delta F_m}{\delta X_2}; \dots; j_{m,n} = \frac{\delta F_m}{\delta X_n}$$

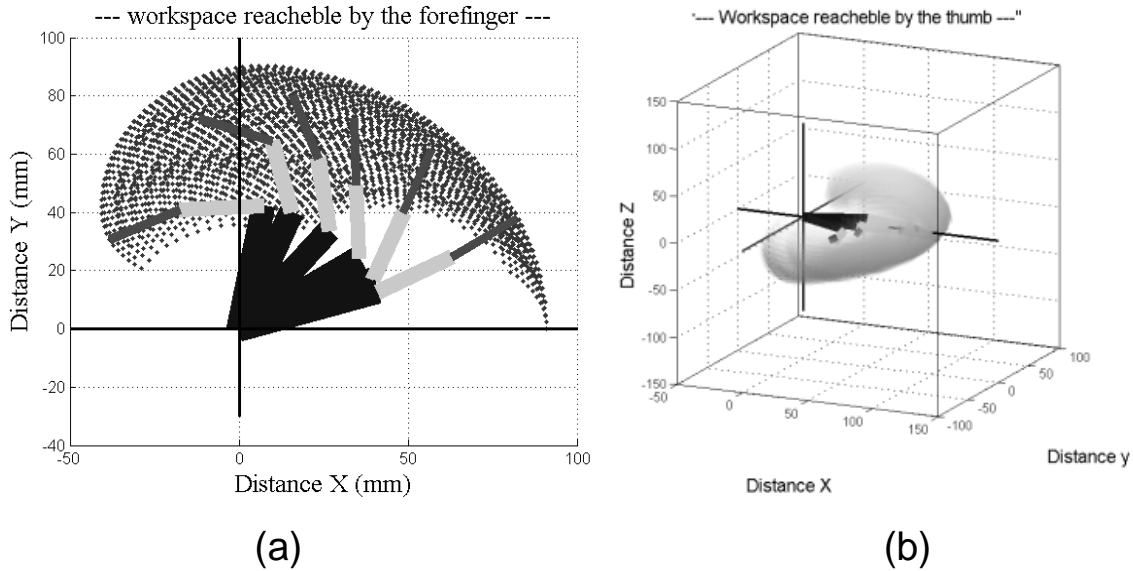


Figure 3. Plot of the ideal workspace for the fingers (a) Forefinger, (b) Thumb.

Table 3. Results of the synthesis of mechanism.

Bar	Forefinger (mm)	Thumb (mm)
R1	10	10
R2	47.5	39
R3	6	11
R4	46	52

RESULTS

Once the synthesis of the mechanisms, in Table 3 the results obtained for the measures used in this work are shown. Finally, using as reference Figure 4a and b, the physical sizing of the links using a Computer Aided Design (CAD) program (Figure 8), whereas during the design process that the measures of the model do not exceed the anthropometric dimensions of the hand. In Figure 5 the prototype made from the methodology outlined here exposed for sizing mechanisms 4 prosthetic hand bars is shown. From the design of the mechanisms, a case study is proposed to evaluate the performance of the entire device, considering as a hypothesis the results shown in Vergara et al. (2012) where it is mentioned that the activity to which he devotes much time the process is feeding. When analyzing Figure 6, the free body diagram is observed during the holding of a water glass with a cylindrical grip power.

To evaluate the performance of the proposed mechanism in this paper, the free-body diagrams shown in Figure 7 were done, while the entire procedure for the calculation of reaction forces is shown in Aguilar (2013), and the obtained values are summarized in Table 4.

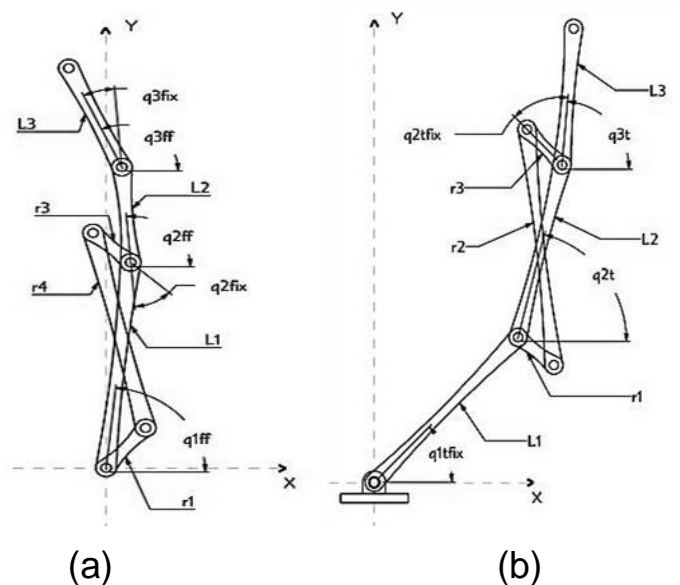


Figure 4. Scheme of the location of the four bar mechanism (a) Forefinger, (b) Thumb.

After determining the loads acting on the complete mechanism due to the case study, we proceed to perform the simulation program for the loads within the finite element calculation, in order to verify the deformation suffered by the pieces, for this the results of static analysis mechanisms were imported, then an automatic meshing part (Figure 8) is created, and finally the stress range at which the material undergoes during the case study is obtained as a result.

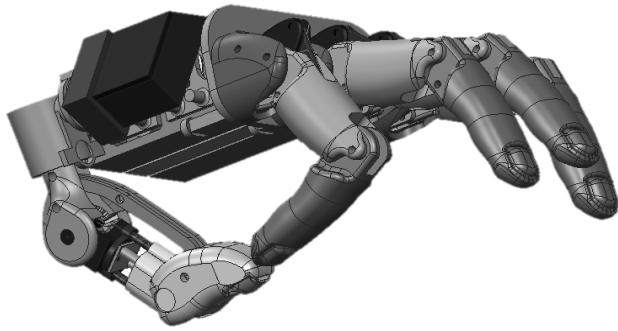


Figure 5. The model of prosthesis of human hand, doing a punctual grip (Aguilar, 2011).

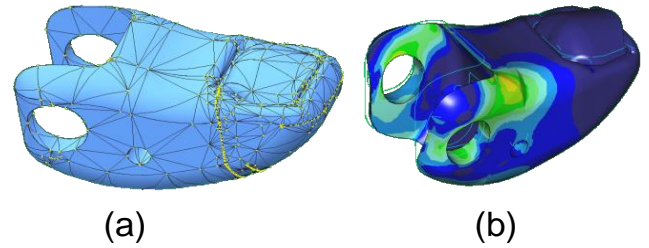


Figura 8. Piece that represent the distal phalanx a) automatic Mesh obtained b) stress field.

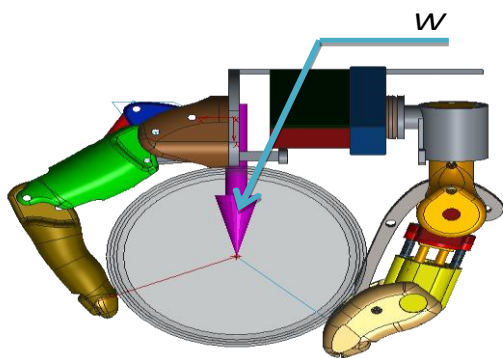


Figure 6. Prototype of the personalized hand prosthesis from the measuring of the anthropometric values.

Table 4. Force applied by the link at the end.

Extremo del eslabón	Fuerza aplicada
A	2.61
B	-1.66
C	44.3
D	43.95

Table 5. Average force exerted by the fingers in certain grips.

Type of grip	Exerted force (N)
Precisiongrip	24-95 N
Lateral grip	37-106 N
Cylindrical grip	
1 finger	30-109 N
2 fingers	7-38 N
3 fingers	23-73 N

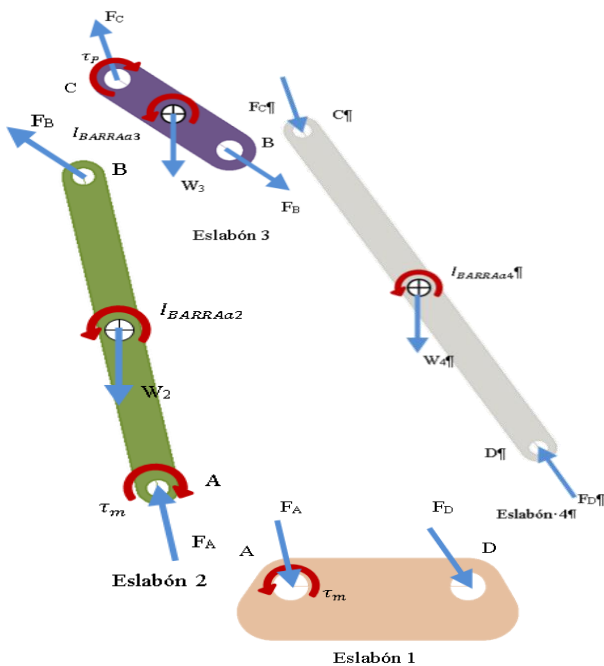


Figure 7. Free body diagrams applied to 4-bar mechanism for the thumb.

DISCUSSIONS

The human hand has 21° of freedom, people generally only have conscious control of about 16. This coupled with the uniqueness of the fingers due to the alignment of the axes of its movement, allows to perform the simplification proposed in this paper given the number of phalanges moving from finger II to V, but such simplification is only valid for prosthesis designs in which generate static grips from sub-actuated mechanisms is planned. The mechanisms calculated in this work are solely responsible for generating flexion movement, leading to define these different locations within the phalanges of the fingers. This is shown in Figure 3a, showing the configuration of the mechanism for the fingers II to V, where the mechanism is located on the first link considered in the kinematic chain of the finger, whereas for the thumb mechanism (Figure 3b) its location is in the second link in the kinematic chain.

This is because it was proposed to split into two coordinated movements the range of flexion and

abduction, as proposed in the description of the opposition movement described by Kapandji and Lacomba (2006), so that the position of the first link only affect the orientation of the second link. For this reason, the position of this link at 45° was fixed, a value according to Cailliet (2006), is designated as the angle at which that section is relaxed thumb, when not performing any flexion.

Furthermore, the research conducted in this paper used the equations of Denavit and Hartenberg so that a mechanism could be synthesized from these equations, but it should be noted that the equation proposed only describes ideal workspace for each finger, which is adapted to a movement pattern that remains within the this workspace, and as presented by Zheng et al. (2011) is possible to improve this equation to define a tangent path to the surface, which would sustain the most common objects of daily use for all activities submitted by Vergara et al. (2012).

Finally, as mentioned in the work of Leal-Naranjo et al. (2013), the four-bar mechanism proposed in this paper is a reduction type of a kinematic chain, which means that the acting force is missing, this can be improved from the use of a kinematic inversion that would modify the position where the force is applied, without having to modify the mechanism already calculated.

Conclusions

Considering the objective of generating flexion and extension moves for the fingers II to V, and allowing to exist a controlled abduction-adduction movement for the thumb, performed automatically by a servomotor. To achieve this throughout this paper, various kinematic relationships were exposed to simplify 14° of the existing freedom degrees of the hand, from which, a methodology for designing kinematic strings of motion was proposed, expressed in terms of the specific anthropometric parameters of the human hand, which is translated in the custom level design prosthetic hand mechanism. Furthermore, the approach undertaken, in mathematical terms, expressed the function to describe the position of the mechanism, which will be used in future studies to develop a control law based on the study of the movement patterns generated by different types of gripping and its relationship with the corresponding myoelectric signal.

Conflict of Interests

The author(s) have not declared any conflict of interests.

ACKNOWLEDGEMENTS


The authors fully appreciate the support granted for this

research work by Instituto Politécnico Nacional and the collaboration of the biomechanics group of the Universidad Politécnica de Madrid for all the support given on the makeover of this work.

REFERENCES

- Alcalde LV, Álvarez ZJM, Bascuas; HJ, García F, Ana A, Germán A, Rubio YCE (2006), La carga física de trabajo en extremidades superiores, los límites del sistema mano-brazo, *Mapfre Seguridad*, 1(101):30-39.
- Aguilar-Pérez LA (2013). Dise- o de una prótesis de dedo pulgar, Instituto Politécnico Nacional.PMCid:PMC3585368
- Belter JT, Dollar YAM (2011). Performance characteristics of anthropomorphic prosthetic hands, *Rehabilitation Robotics (ICORR)*, 2011 IEEE Int. Confer. on pp. 1-7.
- Barrientos AL, Pe-in F, Balaguer C, Aracil, YR (2007). *Fundamentos de robótica*, 2a:93-131.
- Cailliet R (2006). *Anatomía funcional, biomecánica*, 1:152-191.
- Candal MV (2005). Integración CAD/CAE/CAM-PR en la optimización del dise-o de productos plásticos: caso de estudio, *Ciencia e Ingeniería*, 26(3):121-130.
- Cimadevilla LH, Herrera YPJG (2006). Dise-o de un sistema articulado emulando el movimiento de una mano, *Centro Nacional de Investigación y Desarrollo Tecnológico*, P. 125.
- Craig J (2006). *Robótica*. Publisher. Pearson Prentice Hall J3:62-100.
- Chang LY, Matsuoka YY (2006). A Kinematic Thumb Model for the ACT Hand, *Proceedings of the 2006 IEEE International Conference on Robotics and Automation*.
- Deshpande AD, Xu Z, Vande WMJ, Brown;J. Ko BH, Chang LY, Wilkinson DD, Bidic SM, Matsuoka YY (2013). Mechanisms of the Anatomically Correct Testbed (ACT) Hand.
- Feix T, Pawlik R, Schmiedmayer HB; Romero J, Kragic YD (2009). A comprehensive grasp taxonomy, *Robotics, Science and Systems Conference: Workshop on Understanding the Human Hand for Advancing Robotic Manipulation* Cipriani CF, Zaconne G, Stellin;L. Beccai; G. Capiello; M. C. Carroza y P. Dario, *Closed-loop controller for a Bio-inspired multi-fingered underactuated Prosthesis*, IEEE International conference on robotics and automation, 2006.
- Hernández SC, Montoya YMCF (2007). Dise-o de un sistema emulando el movimiento articulado de una mano, brazo y antebrazo, *Centro Nacional de Investigación y Desarrollo Tecnológico*, P. 105.
- Kutz M (2003). *Standard Handbook of Biomedical Engineering. Design*, 6:821-882.
- Kapandji AI. Lacomba YMT (2006), *Fisiología articular: Esquemas comentados de mecánica articular*. Hombro, codo, pronosupinacion, muñeca, mano. 1(6):198-333.
- Leal-Naranjo JA, Torres San Miguel CR, Carbajal-Romero MF, Sáez YLM (2013) Structural numerical analysis of a three fingers prosthetic hand prototype, *Int. J. Phys. Sci.* 8(13):526-536.
- Lewis. FL, Dawson DM, Abdallah YCT (2004). *Robot Manipulator Control: Theory and Practice*.
- Li, ZM, Latash ML Zatsiorsky YVM (1998). Force sharing among fingers as a model of the redundancy problem, *Exper. Brain Res.* 119(3):276-286. <http://dx.doi.org/10.1007/s002210050343>, PMID:9551828
- Li Z-M, Tang YJ (2007). Coordination of thumb joints during opposition. *J. Biomechan.* 40(3):502-510. <http://dx.doi.org/10.1016/j.jbiomech.2006.02.019> PMID:16643926
- Montúfar CPC, Flores JA, García RI, Tapia YHR (2009). *Cinemática de mecanismos y máquinas*, mmmm,---Costa-de-Morais, F. R. J., CAD/CAE/CAM/CIM, (2003), Instituto superior de ingeniería de Porto, P. 123.
- Mirallas MRC, Puig YCM (2000), *Biomecánica clínica del aparato locomotor*, Barcelona; Espa-a, 1:133-169.
- Naik GR, Kumar YDK (2010). Identification of hand and finger movements using multi run ICA of surface electromyogram. *J. Med. Syst.* 36(2):841-851. <http://dx.doi.org/10.1007/s10916-010-9548-2>, PMID:20703649

- Shigley JE, Uicker YJJJ (2001). Teoría de máquinas y mecanismos, 300-325:343-380, 448-480.
- Portilla FÉA, Aviles SOF, Pi-a OR, Ni-o SPA, Moya SE, Molina YVMA (2010). Análisis cinemático y dise-o de un mecanismo de cuatro barras para falange proximal de dedo antropomórfico, Ciencia e Ingeniería Neogranadina, 20-1:45-49.
- Portilla FE, Pi-a OR, Avilés SO, Ni-o SP, Molina YVM (2010). Dise-odel mecanismo actuador de un dedo robot antropomórfico, Revista Facultad de Ingeniería Universidad de Antioquia. 58:153-162.
- Vergara M, Serrano CJ, Rodríguez PJ, Pérez YGA (2012). Resultados de un trabajo de campo sobre agarres utilizados en tareas cotidianas, XIX Congreso Nacional de ingeniería Mecánica. Gregory, R. W., Biomechanics and control of torque production during prehension, The Pennsylvania State University, P. 210.
- Velázquez Sánchez AT (2008) Caracterización cinemática e implementación de una mano robótica multiarticulada, Instituto Politécnico Nacional, P. 326.
- Zollo LS, Roccella E, Guglielmelli M, Carrozza C, Dario PY (2007), Biomechatronic design and control of an anthropomorphic artificial hand for prosthetic and robotic applications, IEEE/ASME Transactions on Mechatronics, 12(4):418-429. <http://dx.doi.org/10.1109/TMECH.2007.901936>
- Zhang X, Braido P, Lee S-W, Hefner R, Redden YM (2005). A normative database of thumb circumduction *in vivo*: center of rotation and range of motion, Human Factors: The Journal of the Human Factors and Ergonomics Society. 47(3):550-561. <http://dx.doi.org/10.1177/154193120504901216>, <http://dx.doi.org/10.1177/154193120504902224>, <http://dx.doi.org/10.1518/001872005774860069>
- Zheng JZ, De La Rosa S, Dollar YAM (2011). An investigation of grasp type and frequency in daily household and machine shop tasks, Robotics and Automation (ICRA), 2011 IEEE International Conference on, pp. 4169-4175.



International Journal of Physical Sciences

Related Journals Published by Academic Journals

- *African Journal of Pure and Applied Chemistry*
- *Journal of Internet and Information Systems*
- *Journal of Geology and Mining Research*
- *Journal of Oceanography and Marine Science*
- *Journal of Environmental Chemistry and Ecotoxicology*
- *Journal of Petroleum Technology and Alternative Fuels*

academicJournals